
DETERMINATION OF LOCAL SURFACE DEFECTS USING A SHACK–HARTMANN WAVEFRONT SENSOR

A.A. GOLOBORODKO, V.I. GRYGORUK, M.M. KOTOV, V.N. KURASHOV,
D.V. PODANCHUK, N.S. SUTYAGINA

UDC 519.2, 620.191.4
©2008

Taras Shevchenko Kyiv National University, Faculty of Radiophysics
(Bld. 6, 2, Academician Glushkov Ave., Kyiv 03127, Ukraine)

A modification of the wavefront registration scheme aimed at improving the spatial resolution of a sensor has been considered. A focused laser beam has been proposed for illuminating a researched surface area; after the optical transformation in a Fourier optics scheme, the beam forms a signal in the sensor plane, which could be considered as a phase image of the surface. The spatial resolution in the surface plane is determined in this case by the sensor aperture, rather than the spatial resolution of the sensor lenslet array. The theoretical analysis and the computer simulation of the wavefront sensor functioning aimed at revealing local defects on the light-reflective surface have been carried out. To reach the submicron spatial resolution of the sensor, the classification of surface microareas is proposed to be made using the methods of multivariate statistical analysis.

1. Introduction

In connection with recent developments in nanotechnologies, the problem of contactless surface diagnostics has become extremely challenging. Optical methods of researches are without a rival, if micron accuracy is required for the determination of surface defects. The capabilities for submicronic defects on the surface to be analyzed by optical methods are restricted by electromagnetic radiation diffraction, which confines the spatial resolution of optical devices in accordance with the relation $R \geq \lambda$, where λ is the radiation wavelength, and R is the linear dimension of a defect. However, this restriction does not mean that optical methods are unsuitable for indicated purposes in general. Certainly, one cannot expect to obtain direct microscopic images of the surface with a corresponding resolution in this case. Nevertheless, the analysis of the scattered field allows one to obtain, in principle,

a qualitative information concerning the presence of submicronic defects.

Recently, the main stream of researches in this area has been aimed at measuring the angular dependence of intensity and the polarization characteristics of the field scattered by a molecular structure of the surface [1, 2]. In this work, we have estimated the capabilities of an alternative method to analyze local inhomogeneities of the surface, which consists in registering the wavefront of coherent optical – in the visible spectral range – radiation reflected from the surface under investigation. In this method, information concerning the phase of radiation is determined directly, so that one may expect that the sensitivity of the method would be higher in comparison with that obtained in the measurements of intensity spectra.

The key feature of the experimental technique proposed in this work is a modification of the conventional scheme for the wavefront registration aimed at improving the spatial resolution [3]. In the traditional scheme of metrological researches making use of a Shack–Hartmann wavefront sensor, the image of the studied surface is projected onto the measurement plane. The operation principle of such a device is well-known [4], and it will not be discussed here. The accuracy of the wavefront reconstruction over the depth usually reaches the value of the order of from $\lambda/20$ to $\lambda/30$.

A significant obstacle for the application of a Shack–Hartmann sensor to the precision monitoring of surfaces is a contradiction between its sensitivity and the spatial resolution. As a rule, the spatial resolution is governed by the dimensions of microlenses in the lenslet array. A reduction of lenslets' diameter results, in practice, in a

reduction of their focal length; hence, it influences the accuracy of the wavefront reconstruction; namely, the accuracy decreases. In this work, a focused laser beam was used for illuminating a local spot on the surface. After the optical transformation, the beam forms a signal, which is the phase image of the surface spot region, in the sensor plane. At the same time, the spatial resolution in the surface plane is governed only by the sensor aperture and does not depend on the resolution of the lenslet array. Certainly, the data obtained in such a way are not enough for the surface relief to be restored immediately, but they are quite sufficient for the statistical analysis of the surface homogeneity to be carried out.

2. Basic Relations

Figure 1 illustrates the process of formation of the secondary field reflected from an inhomogeneity. A probing beam, which is formed by a lens, is reflected from the studied surface and, following this path once again, quits the system.

The amplitude distribution of the probing beam can be written down in the form [5]

$$E_f(\xi, \eta) = \int_{-a/2}^{a/2} E_0 \frac{e^{j\mathbf{k}\mathbf{r}}}{j\lambda f} dx dy, \quad (1)$$

where \mathbf{k} is the wavevector of the incident wave, E_0 the complex amplitude of the primary beam, \mathbf{r} the radius-vector drawn from the lens to the probed plane, f the focal length of the lens, a the entrance aperture (to make calculations simpler, it was considered square), and λ the wavelength. Analytically, the distribution of a complex amplitude in the probed plane can be presented in the form of a Fourier-transform of the optical signal with a constant phase [6],

$$E_f(\xi, \eta) = \frac{a^2 E_0}{j\lambda f} e^{j\left(\frac{2\pi}{\lambda} f + \frac{\pi}{\lambda f} \xi^2 + \frac{\pi}{\lambda f} \eta^2\right)} \frac{\sin \frac{\pi a \xi}{\lambda f}}{\frac{\pi a \xi}{\lambda f}} \frac{\sin \frac{\pi a \eta}{\lambda f}}{\frac{\pi a \eta}{\lambda f}}. \quad (2)$$

Being reflected from a plane surface, the reflected wave remains plane, because the inverse transformation is equivalent to the forward one. However, if the probed plane should contain an inhomogeneity, the reflected wave would include a factor corresponding to the reflection from this inhomogeneity. Consider the reflection from a spherical inhomogeneity, the size of which is R and which inserts an additional phase φ_a

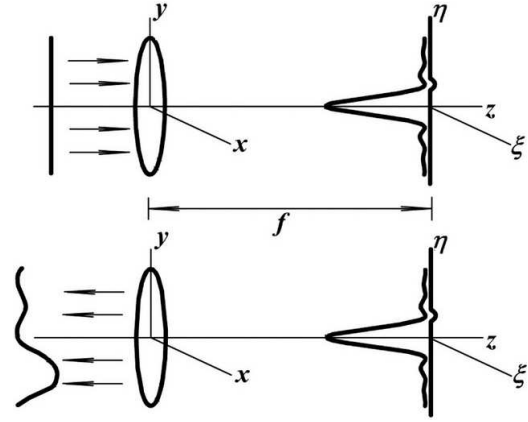


Fig. 1. Process of secondary field formation. ξ and η are coordinates in the probing plane; x and y are coordinates of the input aperture

into the reflected wave:

$$\varphi_a(\xi, \eta) = \frac{k}{2R} (\xi^2 + \eta^2). \quad (3)$$

The amplitude distribution in the reflected wave looks like

$$E_e(x, y) = -E_0 e^{-\frac{jk}{2R}(x^2+y^2)}. \quad (4)$$

Hence, it is evident that the wave is no more plane, and the phase of the reflected wave is, in essence, the image of the surface. It should be noticed that we have considered the case where the radius of the focused spot is less than the characteristic radius of the inhomogeneity. If the size of the focused spot is larger than the characteristic dimension of the inhomogeneity, the reflected wave is – to within the accuracy of the order of $\lambda R^2/a^3$ – the sum of two partial components: a plane wave reflected from a defect-free part of the surface and a wave scattered by the defect. Then, the solution of the diffraction integral is

$$E_e(x, y) = -E_0 \left[\text{rect} \left(\frac{2x}{a}, \frac{2y}{a} \right) + \frac{\lambda R}{a^2} e^{-\frac{jk}{2R}(x^2+y^2)} \right]. \quad (5)$$

Relations (4) and (5) make it evident that the signal in the plane of observation is proportional to the characteristic dimension of the inhomogeneity. It is clear that, while scanning the surface, an inhomogeneity can be revealed by analyzing the wavefront shape. However, in order to determine its center, some integral parameter has to be used. The role of such a parameter can be played by the phase dispersion at the reflected

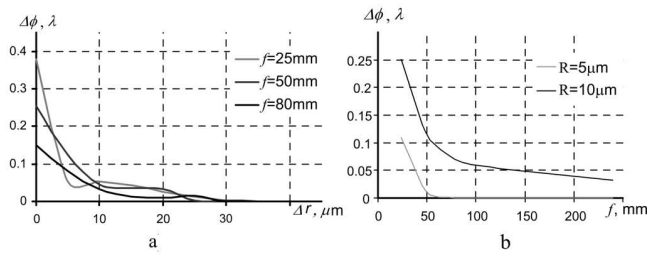


Fig. 2. Dependences of the phase dispersion in the reflected wave (a) on the inhomogeneity position for various focal lengths of forming lens f and (b) on the lens focal length for various characteristic dimensions of inhomogeneity R

wavefront,

$$\Delta\phi = \frac{\lambda \left(\left\langle \arctg^2 \left(\frac{\text{Re}(E_e)}{\text{Im}(E_e)} \right) \right\rangle - \left\langle \arctg \left(\frac{\text{Re}(E_e)}{\text{Im}(E_e)} \right) \right\rangle^2 \right)}{2\pi}, \quad (6)$$

where $\langle \dots \rangle$ means the averaging over the aperture.

In Fig. 2, the dependences of the phase dispersion in the reflected wave on the inhomogeneity position (Δr is the center-to-center distance between the spherical inhomogeneity and the focused beam) and on the curvature radius of the incident wavefront (the curvature radius of a wavefront is proportional to the focal length).

It becomes clear that the phase dispersion in the reflected wave makes it possible to determine the center of the inhomogeneity unambiguously. Moreover, the sensitivity can be controlled by varying the curvature of the wavefront incident on the surface. In the general case, it can be implemented by changing the focal length of the lens that forms the probing beam, as well as by varying the entrance aperture.

Figure 2,b demonstrates that the best sensitivity is achieved in the case where the characteristic dimension of the probing beam is comparable with the size of an inhomogeneity.

3. Experimental Part

In Fig. 3, the optical scheme of the wavefront sensor with enhanced spatial resolution is depicted. This scheme was used to determine defect structures on the surface.

The sample was studied at various incidence angles of a probing beam. At normal incidence, measuring block No. 1 was used. A collimated beam of a He-Ne laser passed through round diaphragm D , then it was split into two beams making use of beam-splitting mirror BS .

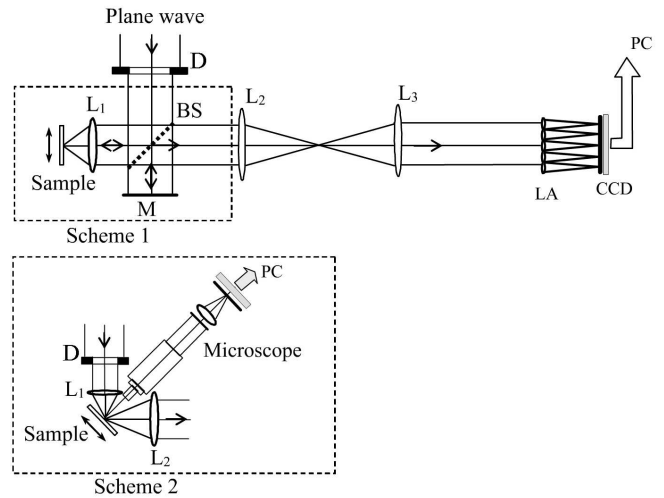


Fig. 3. Optical scheme of a Shack–Hartmann wavefront sensor with enhanced spatial resolution

One of the beams got into microscope objective L_1 , in the focal plane of which there was a sample of the surface under study. The dimensions of the focused spot on the surface could be varied from 5 to 30 μm depending on the size of the working aperture of diaphragm D . The beam, having been reflected from the surface and having passed through microscope objective L_1 once more, formed an object wavefront which was displayed in the plane of refractive lenslet array LA making use of the system of objectives L_2 and L_3 . The dimensions of every array lenslet were $0.4 \times 0.4 \text{ mm}^2$, and its focal length was 24 mm. The other beam, having been reflected from mirror M , formed a plane wavefront which was used for the accurate calibration of array lenslet foci in the plane of a CCD photodetector, the resolution of which was 768×576 pixels, each pixel having the dimensions of $6.3 \times 6.3 \mu\text{m}^2$.

If measuring block No. 2 was used, the incidence angle of a probing beam could be varied in a wide interval (in the experiment, the results of which are given below, this angle amounted to 45°). In this case, a microscope objective with smaller focal length was used as L_1 , so that the size of a focused spot on the plane normal to its optical axis was 3 μm . The sample could be shifted in its plane making use of a two-coordinate micrometric stage. The shift of the sample was monitored with the help of an optical microscope connected to a computer.

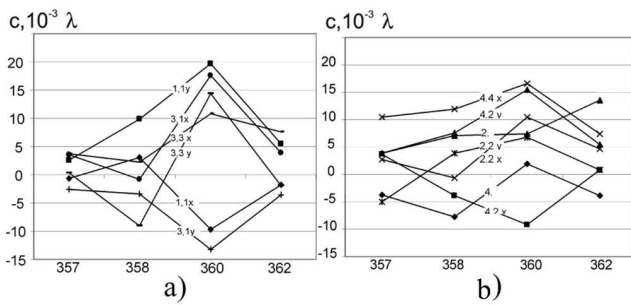


Fig. 4. Expansion of the restored wavefront phase in the basis of Zernike polynomials: expansion coefficients at even- (a) and odd-power (b) polynomials

3.1. SiO₂ Film

In the first series of experiments, the film of polycrystalline silicon chemically deposited in a low-pressure reactor from the gas phase onto the surface of a silicon single crystal covered with a 0.1- μm layer of SiO₂ oxide was selected as a sample for surface researches. The sample was studied as follows. The wavefronts reflected from different sample regions were analyzed. A series of 10 registrations separated by equal time intervals was made for every region in order to take the statistical straggling of data into account.

One of those regions included an apparent defect, which can be observed visually as the anomalous scattering of the focused radiation. Three other regions were statistically homogeneous; at least the difference in dispersion effects or in the forms of wavefronts was not monitored explicitly. A surface structure peculiarity in the defect region was also evidenced for by the analysis of the coefficients of the reconstructed wavefront phase expansion into a series of Zernike polynomials (Fig. 4). One can see that the majority of coefficients for defect region #360 have values different from those for other regions.

It should be noted that the array of local wavefront slope values obtained with the help of the sensor within the limits of a surface microregion and, ultimately, the restored two-dimensional distribution of phases and the set of coefficients obtained at expanding the wavefront in some functional basis can be considered as a collection of certain informative attributes that characterize the surface region under investigation.

Such an amount of input data used in the solution of the surface classification problem makes it reasonable to apply the multivariate statistical analysis. Its essence consists in that a few (2 – 3) principal components which contain as much statistical

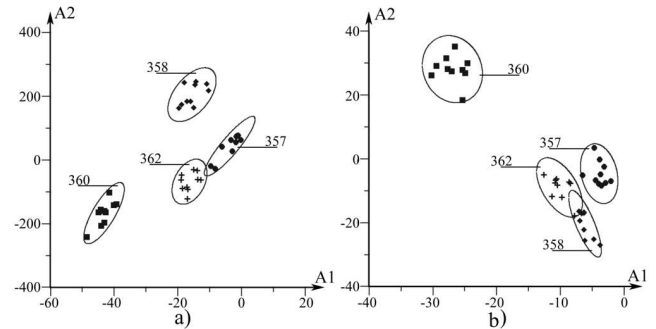


Fig. 5. Diagrams of secondary attributes constructed by (a) the beam displacements and (b) the wave phase distributions

information concerning primary data as possible, are selected from plenty of measured data. The vectors of input data are represented in the space of obtained principal components, so that they can be analyzed both qualitatively (visually) and quantitatively. One of the most widely applied methods to select secondary attributes (the principal components) is the Karhunen–Loève (KL) one [3]. The results of classification by first two expansion coefficients (A_1 and A_2) in the KL basis are exhibited in Fig. 5.

A learning sample was formed from experimental data obtained for all four surface regions. The displacements of spot centroids in the focal plane of lenslets (a 504×504 correlation matrix) were selected as primary data in the first case (Fig. 5,a). In addition to the analysis of spot displacements, the same method was applied to analyze the reconstructed phase fronts (Fig. 5,b, a 154×154 correlation matrix). Provided that the proper basis of the correlation matrix is used, a considerable separation of the data belonging to the “defect”-region-#360 class from all other primary data can be observed in the two-dimensional space of secondary attributes. The diagrams given above for the principal components make it possible to draw conclusions concerning not only the separation or non-separation of individual classes, but also – by examining the distances between corresponding class centroids – about their higher or lower similarity to the reference surface.

The results obtained confirm the efficiency of multivariate statistical analysis for the surface recognition procedure making use of a wavefront sensor, irrespective of whether it is carried out on the basis of directly measured data or special calculated characteristics. Note that the proposed testing technique cannot be used for the straightforward reconstruction of a surface relief. Therefore, all the methods discussed,

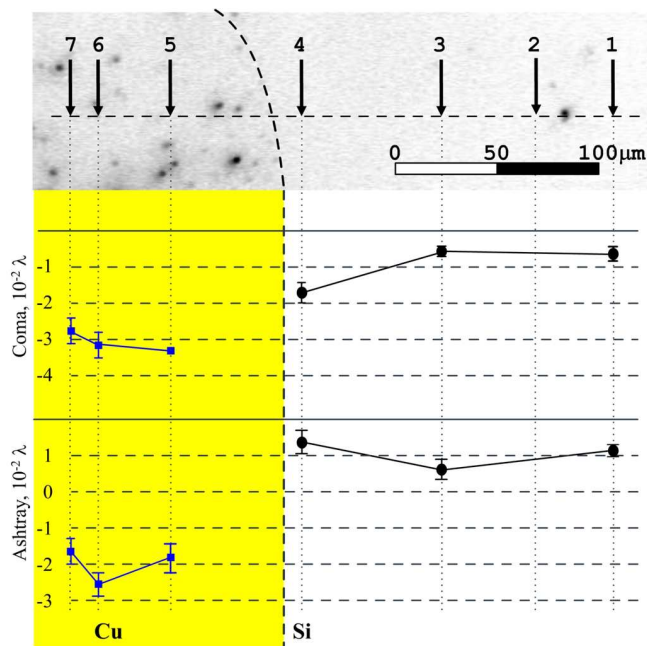


Fig. 6. Image of a fragment on the sample surface (arrows point to tested points) and the values of coefficients in the expansion in Zernike polynomials for various points on the sample surface: (a) aberration Z_7 (coma) and (b) aberration Z_{14} (ashtray)

which are used to form attributes, bring about almost identical results. As a consequence, the displacements of spot centroids can be used directly as primary data. Such a selection makes the procedure of wavefront restoration, which is inherently unstable, unnecessary, but requires that matrices of larger dimensions should be diagonalized.

3.2. Cu–Si Films

The second series of experiments aimed at carrying out a comparative analysis between the wavefronts reflected from the surfaces of different materials possessing different structures. For this purpose, some part of a sample with polycrystalline silicon film was additionally covered with a 100-nm copper layer.

In Fig. 6, we present the image of the surface fragment of a sample under study. The region to the left from the dashed curve is the copper layer, the silicon film is to the right. Point 2 on the silicon film was a reference one: three points (1, 3, and 4) on the silicon surface and three points (5, 6, and 7) on the copper surface were tested with respect to it. Point 4 was located close to the diffuse boundary between those regions. The regions of focusing were

so selected that surface defects should not be observed explicitly.

The estimation was carried out by analyzing the coefficients of the wavefront phase expansion in the basis of Zernike polynomials up to the 6-th order inclusive. In the general case, the distribution of Zernike coefficients was rather stochastic for silicon; but, for the copper film, a correlation between the values of coefficients in all regions was observed.

In Fig. 6, the correlation dependences on the testing point are plotted for two expansion coefficients. One can see that the coefficient values, which correspond to coma aberration for copper, almost are not changed and exceed the corresponding values for silicon (points 1 and 3) by a factor of five, being twice as large for point 4 near the boundary. The difference between point 4 and other points on the silicon film is explained by the fact that this point is practically located at the boundary between two films. For the 4-th order aberration of the “ashtray” type, the coefficients are almost identical by magnitude, but have different signs for different surface sections: positive for silicon and negative for copper. Therefore, a preliminary qualitative analysis of the surface for homogeneity can be carried out by analyzing the magnitude and the sign of the corresponding Zernike coefficients.

4. Conclusions

In the framework of a method aimed at detecting the local surface inhomogeneities making use of the Shack–Hartmann wavefront sensor, we have proposed to use a focused laser beam, which considerably enhances the spatial resolution of the method. A basic capability of the method to register local surface inhomogeneities, whose characteristic dimensions are much less than the diameter of a focused point, has been demonstrated. It has been proved theoretically that the sensitivity of finding an inhomogeneity can be controlled by varying the curvature of the wavefront incident onto the surface. We have proposed to use the multivariate statistical analysis of sensor data in the space of principal components for the classification of individual sections on the surface. Our approach can probably be applied for revealing the micron- and submicron-sized defects on surfaces.

The work was partially supported by the grant No. M/175-2007 of the Ministry of Education and Science of Ukraine.

1. V.A. Sterligov, Yu.V. Subbota, Yu.M. Shirshov, L.P. Pochekeylova, E.F. Venger, R.V. Konakova, and I.Yu. Ilyin, *Appl. Opt.* **38**, 2666 (1999).
2. S.I. Lysenko, B.A. Snopok, V.A. Sterligov, E.V. Kostyukevich, and Yu.M. Shirshov, *Opt. Spektr.* **90**, 678 (2001).
3. M.M. Kotov, V.N. Kurashov, D.V. Podanchuk, T.V. Rodionova, and V.M. Solovyov, *Visn. Kyiv. Univ. Ser. Fiz. Mat. Nauky* N 3, 341 (2006).
4. D.M. Alloin and J.M. Mariotti, in *Adaptive Optics for Astronomy*, edited by D.M. Alloin and J.-M. Mariotti (Kluwer, Dordrecht, 1994), p.269.
5. G.W. Goodman, *Statistical Optics* (Wiley, New York, 1985).
6. M. Born and E.W. Wolf, *Principles of Optics*, 2nd ed. (Pergamon Press, Oxford, 1980).
7. K. Iberla, *Faktorenanalyse* (Springer, Berlin, 1977).

Received 29.02.08.

Translated from Ukrainian by O.I. Voitenko

ВИЗНАЧЕННЯ ЛОКАЛЬНИХ ДЕФЕКТІВ ПОВЕРХНІ СЕНСОРОМ ХВИЛЬОВОГО ФРОНТУ ШЕКА-ХАРТМАНА

*А.О. Голобородько, В.І. Григорук, М.М. Котов,
В.Н. Курашов, Д.В. Поданчук, Н.С. Сутягіна*

Резюме

Розглянуто модифікацію схеми реєстрації хвильового фронту з метою покращання просторового розрізнення сенсора. Запропоновано використовувати для освітлення окремої ділянки поверхні сфокусований лазерний пучок, який після оптичного перетворення в схемі Фур'є оптики формує в площині сенсора сигнал, що можна вважати фазовим зображенням поверхні. При цьому просторове розрізнення в площині поверхні визначається апертурою сенсора, а не роздільною здатністю матриці його мікролінз. Проведено теоретичний аналіз та комп'ютерне моделювання роботи сенсора хвильового фронту з виявлення локальних дефектів відбиваючої світло поверхні. Для досягнення субмікронної просторової роздільної здатності сенсора запропоновано класифікацію мікрообластей поверхні проводити методами багатовимірного статистичного аналізу.